Proceedings of The Institute of Acoustics

THE SCATTERING OF SOUND FROM HEAVILY FLUID LOADED PLATES

D. M. Photiadis

David Taylor Research Center, Bethesda, MD, USA

I. INTRODUCTION

The interaction of acoustic waves with elastic structures is of importance in a wide variety of practical applications. In situations in which the fluid loading, the back reaction of the continuum on the structure, is substantial, we must confront the coupled structural-acoustics problem. Finite nonseparable geometries are particularly troublesome because the fluid loading includes the diffracted field due to the edges. In this paper, we numerically simulate the scattering of a plane acoustic wave from a thin elastic plate, an infinite strip of width "a," under conditions of moderately heavy fluid loading. We give explicit results for both a baffled and unbaffled plate clamped at its edges. We examine these results and compare them to predictions based on simple modeling techniques. This example contains the essential character of more general finite nonseparable geometries, but it is two dimensional and as such easier to solve and understand.

Even for moderately heavy fluid loading an infinite plate is almost transparent. In this frequency range, the reflection coefficient R = (reflected flux/incident flux) is typically of order .01 for a steel plate in water. Unless one is concerned with small deviations from this value, the frequency must be near a resonance of the fluid loaded plate to obtain any interesting far field results. The existence of such phenomena for heavily fluid loaded plates was first noticed by Abrahams[1] who studied a baffled strip, and examined by Crighten and Innes[2] in the same frequency range. Both works give asymptotic low frequency results.

We seek to further our understanding of this phenomena generally, and in particular to answer the question, when are these resonances of importance and how well can we model them using simple techniques? In section II, we give the empirical parameters describing the behavior of the plate near several resonances; the frequencies, effective masses, and radiation efficiencies. We explore how reliably these quantities can be estimated. Of particular interest are the radiation efficiencies since these quantities determine the widths of the resonances and thus their relevance in various phenomena.

I.1 Setting Up the Problem

The fluid parameters are the density ρ and the sound speed c. The plate is characterized by the following parameters: mass per unit area m_p, bending stiffness D, thickness h, and width "a." At frequency ω, the plate supports a bending wave with a wavenumber $k_f = (m_p/D)^{1/4}\omega^{1/2}$ in vacuum. For steady state scattering, there are three relevant length scales; the acoustic wavelength λ_0, the structural wavelength λ_s, and the width of the plate "a." The structural wavelength λ_s is somewhat smaller than the vacuum bending wavelength because of the added mass of the fluid. Thus, there are two dimensionless scales in the problem. We take them to be the phase Mach

number $M = c_f/c = (\omega/\omega_c)^{1/2}$, and $\beta=(c/\omega_c a)=h/a$. For aluminum or steel in water, $\beta=h/a$. Here c_f is the speed of the bending waves in vacuum and ω_c is the coincidence frequency. Other relevant scales are simply expressed in terms of M and β; for example, $k_f a=M/\beta$, $k_0 a=M^2/\beta$. The material properties are conveniently expressed by the fluid loading parameter $\varepsilon = \rho c/\omega_c m_p$. Typically, ε is a small quantity; for steel in water $\varepsilon=.133$, for aluminum in water $\varepsilon=.387$. We consider only the case of steel plates in water, $\varepsilon=.133$.

There have been several ways of defining precisely what heavy fluid loading means. We essentially adopt Crighten's conventions[2]. The fluid loading is said to be moderately heavy at frequency ω if the added fluid mass per unit area on a bending wave is of order the mass per unit area of the plate, m_p. The fluid loading is very heavy if we can neglect m_p relative to the added fluid mass, and light if we may neglect the added fluid mass relative to m_p. In terms of the frequency parameter M, and the fluid loading parameter ε, we have moderately heavy fluid loading for $M\approx\varepsilon$, very heavy fluid loading for $M\ll\varepsilon$, and light fluid loading for $M\gg\varepsilon$. As mentioned above, we consider the case of moderately heavy fluid loading; for steel plates in water this is the regime $.05 \leq M \leq .2$.

The basic equations of motion for the scattering problem can be found in many places[3]. We invert the differential equations using appropriate Green's functions and express them as a boundary integral equation on the plate surface. In this manner, we include the clamped boundary conditions at the edge of the plate. The integral equation thus obtained is a singular Fredholm equation of the second kind. One must treat the singularity with great care, especially in the unbaffled case, but, other than this technical difficulty, the solution is straightforward. In the absence of any particularly convenient set of eigenfunctions, we solved the equations by discretization. The long version of this paper[4] contains the details of these manipulations and the method we used to check the numerical results.

II. RESULTS AND INTERPRETATION

II.1 Unbaffled Plate

We consider only a normally incident plane wave. The reflection coefficient is shown as a function of Mach number for $\beta=.01$ and $\beta=.0064$ in figure 1.

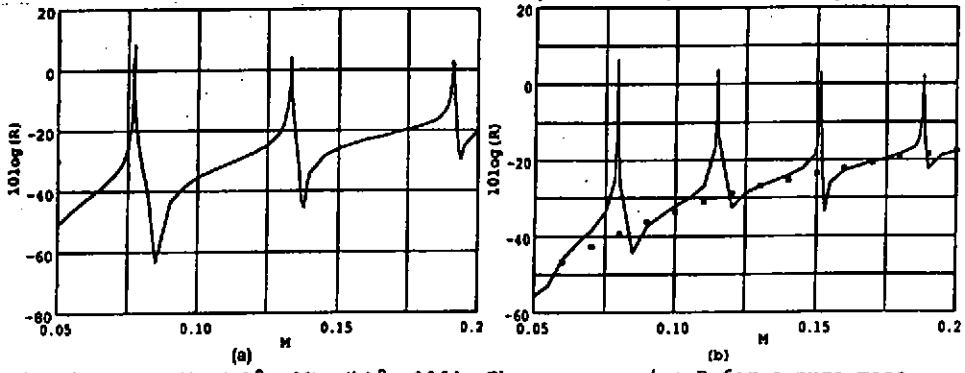

Fig. 1. R vs. M. (a)$\beta=.01$, (b)$\beta=.0064$. The squares give R for a pure mass.

THE SCATTERING OF SOUND FROM HEAVILY FLUID LOADED PLATES

The value $\beta = .01$ corresponds, for example, to a long plate 1mm thick and 10cm wide. We define the reflection coefficient R by

$$R = \frac{\text{reflected power}}{\text{power incident on the plate}}$$

with the power being defined per unit length along the infinite direction of the strip. The quantity $10\log_{10}R$ is shown because the reflection coefficient varies over such a large range. Also shown for comparison for the case $\beta = .0064$ is the reflection from a point reacting impedance with the same mass/area as the plate. The reflection coefficient has huge peaks near the resonant frequencies followed in each case by a minimum. Near the peak, the plate reflects more energy than is directly incident upon it; the plate sucks energy from the adjacent incident field and then reradiates this energy.

The reflection from the masslike impedance of the plate is so small at these low frequencies that the structural vibrations totally dominate the reflected field near the resonances; the enhancement can be as large as 40dB in this example and for a smaller plate or lower frequency even larger. Note however that the width of the peaks is very narrow. The peak reflection coefficient is bounded by the amount of energy that can be absorbed from the acoustic field. Crudely speaking, the plate can grab incident flux which is within a distance of order $\lambda_0/2$. In the above examples we always have $\lambda_0 \geq a$, and thus the maximum effective cross section of the plate is simply the acoustic wavelength. This phenomena, the effective size of the scatterer being given by an acoustic wavelength near resonance, is analogous to the scattering from a simple harmonic oscillator[5] and is also familiar from scattering problems in other fields[6].

The qualitative behavior of the motion away from resonance is quite simple. The velocity field can be understood as a superposition of two components; a forced component as though the plate were infinite, and an oscillating standing wave component due to the edges. The forced motion is almost purely in phase with the incident field because the impedance of the plate is so small compared to ρc. The amplitude of the wavy vibration is $\sim p_i/\rho c$ just as one would have guessed.

The surface wave on the plate is the highly subsonic coupled fluid-plate vibration first mentioned by Junger and Feit[3] and explored in detail in several contexts by Crighten[7]. The wavenumber is accurately predicted by the dispersion relation

$$-i\omega m_p \left\{1 - \frac{k^4}{k_f^4}\right\} - \frac{2i\rho\omega}{\sqrt{k^2-k_0^2}} = 0.$$

Typically, the deviation from the vacuum plate wave number in this frequency range is 20-40% becoming stronger at lower frequencies. For $M \ll \varepsilon$, the very strong fluid loading regime, the mass of the plate becomes negligible relative to the mass loading of the fluid, and the above fifth order equation can be well approximated analytically.

The structure-fluid vibrations typically give rise to only very small effects in the far field due to the weak radiation efficiency of unbaffled structures; the velocity sources near the edge on either side of the plate tend to cancel one another. Just above the surface of the plate, the normal velocity field in the fluid of course coincides with that of the plate,

obeying a clamped boundary condition at the edge of the plate. As we move off the plate the velocity field peaks sharply, corresponding to nearly incompressible flow around the edge of the plate. This effect tends to cancel the net scattering sources of the plate. For light fluid loading, we crudely expect the suppression of the radiated power due to this "short circuiting" to be order M^2; for such small values of M a very strong suppression indeed.

As we approach a resonance, the magnitude of the standing waves becomes large and begins to significantly increase the scattering. As we pass through the resonance, there is an interference effect between the driven and resonant response accounting for the asymmetric shape of the reflection coefficient. For frequencies below resonance, the driven response and resonant response are in phase and their effects add. As we pass through the resonance frequency the resonant response undergoes a phase shift of π radians and now destructively interferes with the driven response; this accounts for the minima located just after each resonant peak.

The peak in total reflected power thus does not yield precisely the resonance frequency although it is quite close to it. The correct indicator is the magnitude of the mean square velocity field. The curves for $\langle v^2 \rangle$ have usual symmetric resonance shapes and we have determined the resonance frequencies and widths from these curves.

The resonance frequencies for the heavily fluid loaded clamped plate are given quite accurately by the formula

$$k_a a - \phi = n\pi,$$

with k_a the fluid loaded wavenumber as given above and $\phi = .37\pi$ a nearly constant phase shift. This form was first given by Crighten and Innes[2] and Abrahams[1] for $M \ll \varepsilon$. We employ the same form and agree surprisingly well on the value of ϕ; they obtain $\phi = 3\pi/10$ in the asymptotic low frequency limit. The phase shift differs by only a small amount from the vacuum value $\phi_{vac} = \pi/2$, and the associated anomolous frequency shift will usually be very small. The resonances given are only the symmetric modes.

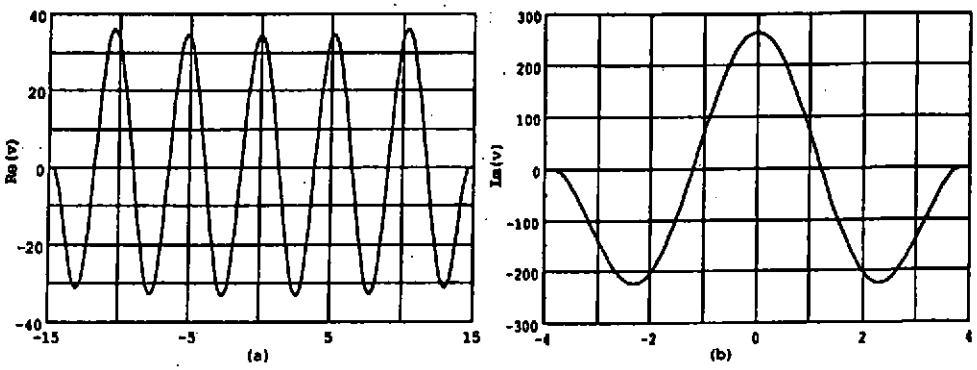

Fig. 2. Unbaffled Mode Shapes. (a) $\beta = .0064$, n=11, (b) $\beta = .01$, n=3

Figure 2 shows some representative plate velocity fields near two of the resonances. We have scaled the velocities to the characteristic fluid

velocity $p_i/\rho c$. These curves are reasonably similar to vacuum mode shapes. Generally, for the lower modes, n=3,5,7, the difference can be interpreted as a small almost uniform offset; i.e. the vibration looks more like A + $B\cos(k_g x)$ than a pure cosine. For the higher modes, it becomes clear that this offsetting is larger near the edges. These changes in the mode shape are important, because small changes in the mode shape can produce a large change in the radiation efficiency of the vibration, and thus in the importance of such phenomena.

II.2 Baffled Plate

For the baffled case it is simpler to consider the transmission coefficient T defined in the natural way,

$$T = \frac{\text{transmitted power}}{\text{power incident on the plate}}.$$

The transmission coefficient is shown as a function of Mach number for $\beta=.02$ and .0064 in figure 3. The peaks are once again due to the symmetric resonances of the plate-fluid system and are immediately preceded in each case by a strong minimum. Near the resonance frequencies the plate absorbs more energy from the acoustic wave than is geometrically incident upon it, T>1, and reradiates this energy. The peak transmission is bounded as in the unbaffled case by the amount of energy the plate can absorb from the incoming field.

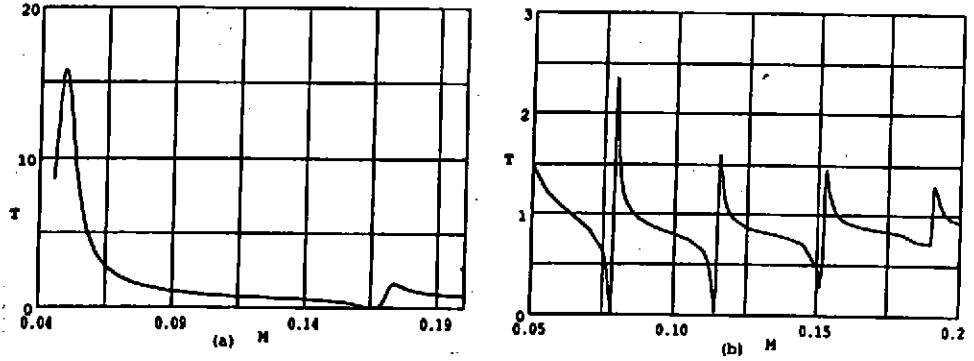

Fig. 3. T vs. M. (a)$\beta=.02$, (b)$\beta=.0064$.

The qualitative behavior of the surface velocity fields is quite similar to the behavior in the unbaffled case. The response is composed of short wavelength oscillations with amplitude $O(p_i/\rho c)$ superposed on an almost uniform driven response. The effects of the fluctuations again tend to cancel in the far field. We expect that the suppression due to this cancellation is a factor of $\approx(\lambda_s/\pi a)$; this is the typical size of pressure fluctuations in the far field. Unlike the unbaffled case, the real and imaginary parts of the velocity field are comparable. This is due to the large radiation damping in the baffled geometry.

The resonant response never dominates the transmitted field because a substantial portion of the available energy is always transmitted. In

addition, the resonances have much lower peaks because of the greater radiation damping. Interference between the driven response and the resonant response accounts for the shape of the transmission coefficient just as in the unbaffled case.

The resonant frequencies for the clamped baffled plate can once again be predicted from the formula

$$k_a a - \phi = n\pi.$$

Here however, ϕ increases slowly with frequency, $.29\pi < \phi < .39\pi$ and for the fundamental mode the phase shift is much smaller, $\phi = .15\pi$. Our results differ with those given by Crighten and Innes[2], they give $\phi = -3\pi/2$. This may be due to the asymptotic low frequency range they consider.

II.3 Resonance Behavior

In this subsection we investigate the characteristics of the resonances for both the baffled and unbaffled configurations. In both cases, near resonance we may approximate the velocity on the plate as

$$v(x) \approx v_n \varphi^n(x) \quad \text{with } v_n = \frac{f_n}{-im_n\omega(1-(\omega_n/\omega)^2)+\eta_n}$$

where $\varphi^n(x)$ is the mode shape, ω_n is the resonance frequency, f_n is the modal force, m_n is the effective modal mass, and η_n is the modal damping, the radiation damping per unit area. One should add to this formula the infinite driven response if an accurate result is needed.

We define the radiation efficiencies of the modes in the standard way,

$$\Pi_{rad} = R_{rad}\langle v^2\rangle \quad \Rightarrow \eta_n = R_{rad}/a$$

For the unbaffled configuration, there is no confusion in separating forced from resonant response since the resonances are so dominant; we obtain the radiation efficiencies in a straightforward manner from our results. For the baffled case, because of interference effects, one cannot obtain accurate values for the η_n in this manner; typically, the radiation efficiency varies by as much as a factor of two over the width of the resonance. For this reason, in the baffled geometry, we computed the response to a line drive at x=0, and determined the radiation efficiencies from these calculations. We thus determine the appropriate values of the η_n in the above formula. The other parameters, f_n and m_n, can be determined easily from the widths and peaks of the resonances. In tables 1 and 2 , we give the defining characteristics for each of the resonances; the resonance frequency, the radiation efficiency, the Q, the effective mass, and the peak value of $|v|$. These quantities, together with the above expression, enable one to crudely estimate the importance of the resonances for the particular narrow band or broad band application of interest. We scale the dimensionful quantities as follows: η_n to ρc, m_n to m_p, and $|v|$ to $p_1/\rho c$.

n	M_n	η_n	Q_n	m_n	$\lvert v\rvert_n^{max}$
β=.0064					
5	.079128	2.2e-4	825	3.85	193
7	.11470	5.7e-4	546	3.15	89
9	.15128	9.0e-4	515	2.69	65
11	.18850	1.25e-3	483	2.26	50
β=.01					
3	.07708	3.42e-4	532	4.075	198

5	.13312	1.4e-3	263	2.75	60
7	.19118	2.6e-3	242	2.28	37
β=.02					
1	.05845	4.35e-4	390	6.67	325
3	.1729	6.2e-3	88	2.433	29

Table 1. Resonance characteristics for the unbaffled plate.

n	M_n	η_n	Q_n	m_n	$\|v\|_n^{max}$
β=.0064					
5	.0786	4.1e-3	42	3.69	33
7	.1148	5.6e-3	50	2.82	23
9	.1522	7.4e-3	56	2.40	18
11	.1902	1.05e-2	48	1.83	11.5
β=.01					
3	.0750	8.6e-3	21	4.23	28
5	.1320	1.2e-2	28	2.54	15
7	.1910	1.7e-2	35	2.15	11
β=.02					
1	.0490	8e-2	2.8	12.2	18.8
3	.1710	4.4e-2	12	2.43	8.4

Table 2. Resonance characteristics for the baffled plate.

III. DISCUSSION

How well can we determine the above parameters describing the resonance behavior using simple modeling techniques? Suppose, for simplicity, we take the vibrational shape to be a vacuum simply supported mode shape,

$$\varphi^n(x) = \sqrt{2}\cos(n\pi x/a).$$

We already have the resonance frequencies with the knowledge of the single phase shift ϕ from the previous section. We now give simple estimates based on this mode shape for the other parameters describing the resonances. It is convenient here to use the actual phase Mach number, $M'=c_s/c=M(k_f/k_s)$.

The modal mass is a distributed effect and should be reasonably independent edge effects and boundary conditions; the infinite plate result is

$$m_n = m_p + 2\rho/k_n = m_p\left(1 + \frac{2\varepsilon}{M'_n}\right).$$

We expect that this approximation will only be good for the higher order modes, but in fact it works reasonably well down to n=3. We can derive separate formulae for the added mass on the n=1 mode using standard techniques.

The radiation efficiency will be sensitive to the boundary conditions and edge effects; herein lies the largest and most important difference between baffled and unbaffled geometries. It is straightforward and familiar to derive the radiation efficiency of the baffled plate[3,8], we give only the result. For the unbaffled plate, notice the following. From the equation of motion for the plate, the assumed form of the velocity field, and the dispersion equation for k_s, we can determine the surface pressure field[9],

$$p_s = i\rho c\,(k_0/k_s)\cos(k_s x) = i\rho c\, M'\, v(x).$$

From this, we determine the radiation damping per unit area,

$$\eta_n^{ubaff} = \frac{\rho c}{k_n a} M'^3 (1+2J_1(k_0 a)/k_0 a)$$

THE SCATTERING OF SOUND FROM HEAVILY FLUID LOADED PLATES

$$\eta_n^{baff} = \frac{\rho c}{k_n a} 2M'(1+J_0(k_0 a)).$$

The functional forms are characteristic of two line sources spaced a distance "a" apart as we would expect. We should multiply these formulae by 2 if we want results for a clamped plate[10].

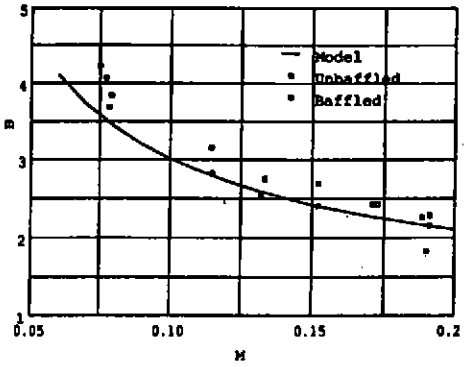

Fig. 4. Effective Masses vs. M For the Resonances

The modal force can be evaluated with similar ease in the baffled geometry, but for the unbaffled case we have finally found trouble with straightforward methods. It can however be determined using an elegant reciprocity argument due to Preston Smith[11]. The result is

$$f_n = 2\sqrt{D(\theta)\eta_n/k_0 a}$$

where $D(\theta)$ is the directivity function of the radiation from the excited mode, and θ is the angle of incidence of the incoming plane wave.
We now make reasonable guesses for $D(\theta)$. For the unbaffled case we take $D(\theta)=2\cos^2(\theta)$, dipole directivity, and for the baffled case $D(\theta)=1$, monopole directivity. We are surely underestimating $D(0)$ in the baffled case, the radiation is somewhat directive, and we are making some error in the unbaffled case as well. However, because of the square root, the errors due to this tend to be relatively small. Using the empirical results for η_n and f_n as a test, we find the above relationship to hold reasonably well. The error is typically only a few percent and in all cases less than 30%. As expected, we tend to underestimate because of our crude guess for the directivity.

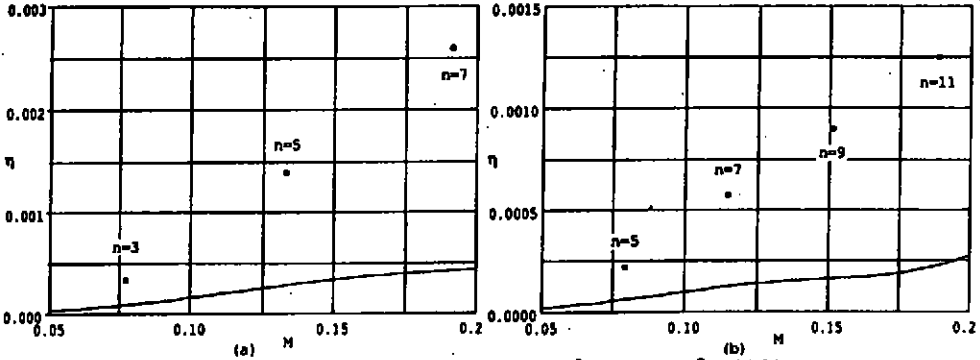

Fig. 5. Unbaffled Radiation Efficiencies. (a)β=.01, (b)β=.0064

We thus have only to compare the effective masses and the radiation efficiencies of the resonances. In figure 4, we show the masses for the various resonances versus the model prediction. The agreement is fairly

good; the added mass is indeed only weakly dependent on edge effects. The radiation efficiencies are shown versus the model predictions in figures 5 and 6. In this quantity there can be substantial, order of magnitude, deviations between the simple modeling predictions and the simulated results.

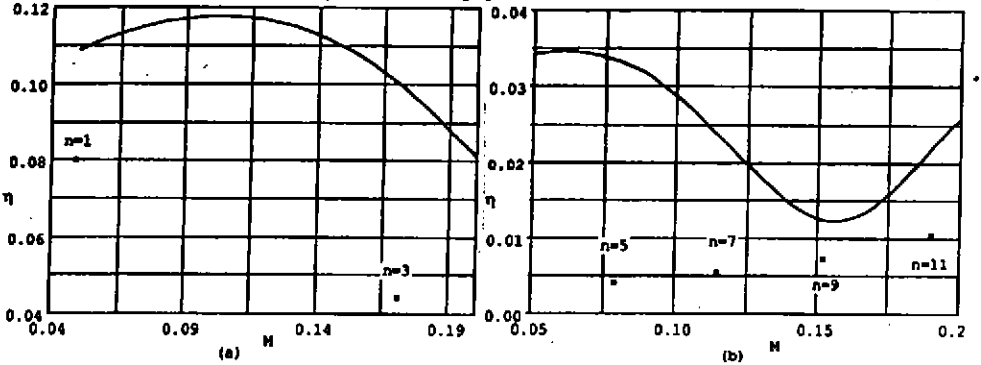

Fig. 6. Baffled Radiation Efficiencies. (a)β=.02, (b)β=.0064

This is due to the influence of the heavy fluid loading on the vibrational shapes. The striking result is that for the baffled geometry we tend to overestimate the radiation efficiencies, while for the unbaffled geometry we tend to underestimate the radiation efficiencies.

These results can be explained by the following rule we conjecture: in the presence of fluid loading, the vibrational shape adjusts itself in order to reduce the interaction between the structure and the fluid; i.e. to reduce the power flow between the structure and the fluid. In the baffled case, because of the high radiation efficiency, the part of this power flow which gets radiated to the far field is comparable to the reactive part, and tends to get reduced when we reduce the net interaction between the plate and the fluid. In the unbaffled geometry, the energy which escapes to the far field is negligible relative to the reactive energy. The tendency here is to reduce the short circuiting flow around the edges of the plate which in turn increases the radiation efficiency. If valid generally, this principle can give us more insight into the dynamics of heavily fluid loaded structures[12].

The comparison of the simulated results with the simple modeling predictions enables us to more fully understand the effects of heavy fluid loading. There are basically two effects, a substantial mass loading, and a small change of the vibrational shape in the vicinity of the edges. The mass loading is straightforward to approximate and can give rise to a sizable shift of the resonance frequencies. The change of the mode shapes gives rise to a small frequency shift, but a large, as much as order of magnitude, change in the radiation efficiencies of the resonances.

I would like to thank the many individuals at DTRC who have discussed this problem with me and given me great encouragement.

References

[1] I.D. Abrahams, Proc. R. Soc. Lond. A378, 89-117 (1981)

[2] D.G. Crighten and D.Innes, Phil. Trans. R. Soc. Lond. A312, 295-341 (1984)
[3] D.Feit and M. Junger, *Sound, Structures, and their Interaction*, MIT (1972)
[4] Submitted to the Journal of Sound and Vibration
[5] E. Meyer and E. Neumann, *Physical and Applied Acoustics*, Academic Press (1972)
[6] See for example, K. Gottfried, *Quantum Mechanics Vol.1*, W.A. Benjamin (1966)
[7] For example, D.G. Crighten, The Free and Forced Waves on a Fluid Loaded Plate, Journal of Sound and Vibration 63(2), 225-235 (1979)
[8] G. Maidanik, JASA 34(6), 809-826 (1962)
[9] To my knowledge, this simple method has not been employed previously.
[10] P.W. Smith, JASA 36(8), 1516-1520 (1964)
[11] P.W. Smith, JASA 34(5), 640-647 (1962)
[12] We envision here a minimum principle with several competing terms, the "interaction term" becoming more important for heavy fluid loading.

SPANWISE WALL-CURVATURE EFFECT ON THE LOW-WAVENUMBER SINGULARITY OF THE TURBULENT BOUNDARY LAYER WALL PRESSURE SPECTRUM

M R Dhanak

Topexpress Limited, Cambridge, England

This paper is concerned with the characteristics of the pressure fluctuations induced on a rigid cylindrical surface by a statistically stationary turbulent boundary layer. In particular, the effect of spanwise curvature on the low wavenumber characteristics of the cross spectral density of surface pressure is examed using Lighthill's acoustic analogy.

The pressure fluctuations induced by a turbulent boundary layer have frequencies, ω, which typically lie in the range $O(U/\Delta) - O(U/\delta)$, where Δ is the boundary layer thickness, δ is the viscous sublayer thickness and U is the speed with which the boundary layer eddies convect. The fluctuations induce self noise, cause structural vibrations and radiate sound.

For flow over a plane surface at low Mach numbers $M = U/c$, where c is the speed of sound, a typical plot of the cross spectral density of wall pressure against streamwise wavenumber (Figure 1) features a broad peak at the convective streamwise wavenumber $O(\omega/U)$ together with a relatively narrower peak at the acoustic (lower) wavenumber $|\kappa| = \omega/c$, where κ is the total surface wavenumber. The breadth of the convective peak is associated with the range of eddy sizes in the turbulent boundary layer which contribute to the hydrodynamic pressure fluctuations. The acoustic peak is narrower since the wavelength associated with the radiated noise from an isolated eddy is expected to be $O(M^{-1})$ times longer than the typical eddy size. The two peaks are fairly well apart and it makes sense to consider the characteristics of the spectral density in the vicinity of each separately. The characteristics of the pressure spectrum in the vicinity of the convective peak are principally governed by incompressible mechanics, while the low-wavenumber characteristics for $|\kappa| < \omega/c$, are governed by the effects of compressibility. Here, we shall mainly be concerned with the latter. For a fixed frequency, the length scales associated with low wavenumber considerations are large compared with those associated with viscous diffusion so that the fluid may be regarded as inviscid.

The surface pressure spectrum is determined using the Lighthill formulation (1952). According to this, if the surface is plane and of infinite extent, the spectral density of surface pressure has a non-integrable singularity at the acoustic wavenumber, the spectral density being proportional to the response function $|\omega^2/c^2|\kappa^2 - \omega^2/c^2|^{-1}$. Thus for a given non-zero frequency, the contribution to the correlation area from the low wavenumber domain of the wavenumber plane is infinite! This paradoxical result arises because no allowance is made in the formulation for the weak interaction of the sound field of a turbulent source element with the turbulence through which it propagates so that it does not decay fast enough with distance for the integrated contribution from distant acoustic sources in the infinite plane to be finite. Although damping of the sound field due to turbulence is a slow process, over a distance $O(M^{-2}\lambda)$ where λ is the wavelength of sound, it is

significant enough to make the integrated contribution bounded (Crow (1967)); the effect of viscous surface shear also acts over a comparable distance (Howe (1979)). At low Mach numbers, the distances involved are rather large and if the turbulent boundary layer extends over a region with typical dimension $L \ll M^{-2}\lambda$, the damping can be ignored and the neglect of interaction of sound with turbulence in Lighthill's formulation is justified. For a finite value of L (Ffowcs Williams 1965, 1982; Bergeron 1973; Howe 1987), the singularity at the acoustic wavenumber is integrable. Away from the acoustic wavenumber, $|\kappa^2 - \omega^2/c^2| \gg \omega/cL$, the spectrum coincides with that for the infinite plane. The coefficient of the point pressure spectrum is proportional to $\log(\omega L/c)$.

Here we consider a turbulent boundary layer flow over a smooth infinitely long rigid cylinder of radius a and determine the associated cross-spectral density of surface pressure using the Lighthill formulation (c.f. Dhanak (1988)). Our principal aim is to investigate how the cylindrical geometry may modify the nature of the power spectrum in the vicinity of the acoustic wavenumber from the known form for a plane rigid surface in the absence of any acoustic damping by turbulence or viscosity. The turbulent boundary layer is assumed to be statistically stationary, transient motions based on initial conditions having decayed away. An expression for the cross power spectral density of surface pressure is obtained in terms of a product of a response function associated with the cylindrical geometry and a term essentially involving the source functions; viz.,

$$P^*(k,n,\omega) = \rho_0^2 U_c^3 \Delta^5 \left| \frac{K_n(\gamma a)}{\gamma K_n'(\gamma a)} \right|^2 R(k,n,\omega)$$

where ρ_0 is the fluid density, K_n are modified Bessel functions, $\gamma^2 = k^2 - \omega^2/c^2$ and R contains the source terms. In the appropriate limit of letting the radius of the cylinder become infinite, this expression reduces to the corresponding expression for an infinite plane surface.

For a cylinder, the radiative domain corresponds to the strip $|k| \le \omega/c$, where k is the streamwise wavenumber (see Figure 1). For low wavenumber considerations, the term involving the source functions is expected to be well-behaved (see Bergeron, 1973) and the nature of the spectrum is principally governed by the response function. If n/a denotes the azimuthal wavenumber, then for $n/a = 0$, the response function has a logarithmic, integrable, singularity at the acoustic wavenumber. For $n/a \neq 0$, the response function has finite peaks at $\kappa = \pm\kappa_m$ where $\omega^2/c^2 - n^2/a^2 > \kappa_m^2 > \omega^2/c^2$; the peaks become broader and lower with increasing value of n/a. Away from the peaks, the response function is well-behaved and decays to zero as $|\kappa| \to \infty$. Thus, again in contrast to the case of the infinite plane surface, the low wavenumber contribution to the point spectrum is finite.

It is shown that for a cylinder of large radius ($a \gg c/\omega$), the coefficient of the peak value of the pressure spectrum is proportional to $M^4(\omega a/U)^2 n^{-4/3}$ and the width of the peak is $O(n^{2/3}/a)$. Further, away from the peak, the spectrum coincides with that for an infinite plane surface. This suggests that for an

almost plane cylinder, the effect of finite curvature may be allowed for by approximating the response function by $\omega^2/c^2(|\kappa^2(1-\beta^2) - \omega^2/c^2| + \kappa^2\beta^2)^{-1}$ where β is $O((\omega a/c)^{-1/3})$ and varies with the wave-vector angle. Then, for non-zero values of n/a, the response function has a peak value β^{-2} and peak width $O(\beta)$. For n/a = 0, the approximate response function is singular at the acoustic streamwise wavenumber. However, the low-wavenumber contribution to the point spectrum is finite, being $O(\rho_0^2 U_c^3 \Delta M^4 \log((\omega a/c)^{2/3}))$. This contribution corresponds to that from equivalent turbulent sources distributed over a finite plane disc of radius $L = O(a^{2/3}(\omega/c)^{-1/3})$. For this value of L, L^{-1} is the exponential decay rate of creeping rays on a cylinder (Jones (1979)). Thus the point pressure spectrum is finite, the dominant low wavenumber contribution to the point spectrum being due to creeping rays emanating from turbulent sources within a distance L (measured along the surface of the cylinder) of the point. It may be noted that the contribution implied by ray theory from sources in line of sight of the point corresponds to that from equivalent sources distributed over a plane disc of smaller radius $L = O(\sqrt{a\Delta})$, $\omega\Delta/c$ being very small for low Mach number flows. Hence, in approximating the low wavenumber contribution to the point spectrum or sound intensity it is insufficient to consider individual contributions merely from turbulent sources directly in line of sight of the point; the creeping ray contribution from sources out of the line of sight also needs to be considered, it being the dominant contribution.

The results are consistent with that obtained, independently, by Howe (1987) who considered the effect of general surface curvature (in both streamwise and transverse directions), on the singularity at the acoustic wavenumber. Having identified the dominance of the creeping ray contribution to the spectral peak at the acoustic wave number, he evaluates the leading order effect of general wall curvature. One consequence of having a general curvature is that the logarithmic singularity corresponding to axisymmetric spectral elements in the case of a cylinder, referred to above, is removed and the spectrum is finite everywhere.

It is shown that the intensity of radiated sound for turbulent flow past a cylinder of large radius can be estimated as

$$I = O\left(\rho_0 \frac{U_c^8}{c^5} \log(Ma/\Delta)\right).$$

This work was carried out with the support of the Procurement Executive, Ministry of Defence.

References

Bergeron, R.F. Jr., 1973, Aerodynamic sound and the low-wavenumber wall-pressure spectrum of nearly incompressible boundary layer turbulence. JASA, 54, p123

Crow, S.C., 1967, Visco-elastic character of fine-grained isotropic turbulence, Phys. Fluids, 10, 1587-1589.

Dhanak, M.R., 1988. Turbulent Boundary Layer on a circular cylinder: the low-wavenumber surface spectrum due to a low-Mach-number flow. To appear in J. Fluid Mech.

Ffowcs Williams, J.E., 1965, Surface-pressure fluctuations induced by boundary layer flow at finite Mach numbers. J. Fluid Mech., 22, p507

Ffowcs Williams, J.E., 1982, Boundary-layer pressures and the Corcos model: a development to incorporate low-wavenumber constraints. J. Fluid Mech., 125, p9

Howe, M.S., 1979, The role of surface shear stress fluctuations in the generation of boundary layer noise. J. Sound Vib., 65, pp159-164.

Howe, M.S., 1987, The singularity at the acoustic wavenumber of the turbulent boundary layer wall pressure spectrum. Proc. R. Soc. Lond. A412, 389.

Jones, D.S., 1979, Methods in Electromagnetic Wave Propagation. Oxford: Clarendon Press.

Lighthill, M.J., 1952, On sound generated aerodynamically. I. General Theory. Proc. Roy. Soc. Lond. A211, 564-587.

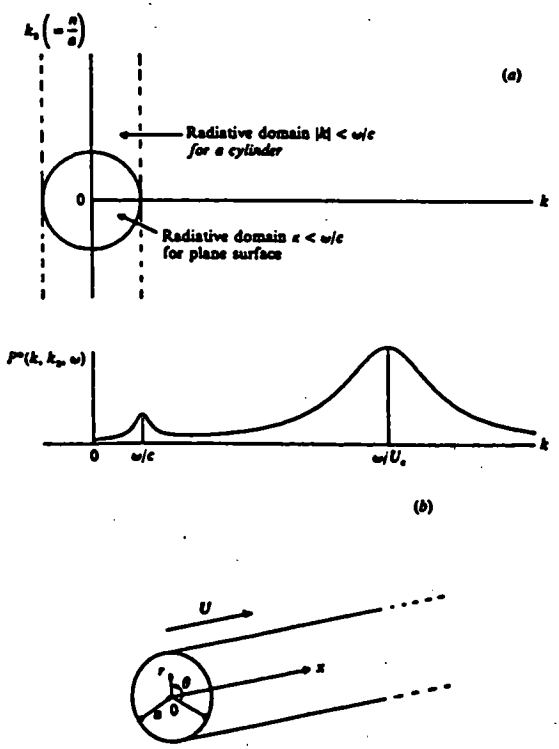

FIGURE 1. (a) Typical fixed-frequency cross-spectral density of pressure on a plane surface with $k_3 = 0$. The radiative domains in the wavenumber plane for the plane surface and for a circular cylinder are shown above. (b) The coordinate system.